PHYSICAL REVIEW C **77**, 051302(R) (2008)

Structure in $E1$ strength distribution built on the 15.1 MeV $T = 1$ state in ^{12}C

D. R. Chakrabarty,[1,2] V. M. Datar,[1,2] Suresh Kumar,[1] E. T. Mirgule,[1] A. Mitra,[1] V. Nanal,[3] and P. C. Rout[1,2]
[1]*Nuclear Physics Division, Bhabha Atomic Research Centre, Mumbai 400 085, India*
[2]*Homi Bhabha National Institute, Bhabha Atomic Research Centre, Mumbai 400 085, India*
[3]*Tata Institute of Fundamental Research, Mumbai 400 005, India*
(Received 27 December 2007; published 27 May 2008)

The measurement of the giant electric dipole resonance built on the isobaric analog state in the self-conjugate even-even nucleus ^{12}C is reported covering a wide excitation energy range. This is done using the ^{11}B(p, γ) reaction leading to the 15.1 MeV $T = 1$ state in ^{12}C over a proton energy range of 7 to 24.5 MeV. Two resonances of 1.3 and 2 MeV widths are observed at excitation energies of 24.4 and 28.8 MeV superimposed on a smoothly varying cross section. The γ transitions from both the resonances are assigned $E1$ multipolarity. The structured $T = 0$ component of the $E1$ strength distribution is thus very different from that built on the first $T = 1$ state in the neighboring nucleus ^{14}N and those built on the ground states of ^{12}C and ^{14}C.

DOI: 10.1103/PhysRevC.77.051302 PACS number(s): 24.30.Cz, 25.40.Lw, 27.20.+n

The giant electric dipole resonance (GDR) built on isobaric analog states (IAS) is an interesting mode of excitation in nuclei. This has been studied using the pion double charge exchange reactions in a number of nuclei [1]. Radiative capture reactions leading to the states of isospin $T = T_3 + 1$ is another way of exciting this mode. Here $T_3 = (N - Z)/2$, N and Z being the neutron and the proton numbers of the final nucleus. For odd-odd $T_3 = 0$ nuclei, the first $T = 1$ state appears at a low excitation energy enabling a singles γ-ray measurement to resolve the transition to this state. To our knowledge, however, the only case studied so far is the GDR built on the $T = 1$ state in ^{14}N via ^{13}C(p, γ) reaction [2].

The first $T = 1$ state in even-even $T_3 = 0$ nuclei appears at a high excitation energy. For example, in ^{12}C this state, which is the IAS of the ground states of ^{12}B and ^{12}N, is at 15.1 MeV. Thus a singles measurement of the proton radiative capture is extremely difficult due to neutron induced background and pileup effects. No measurement on the GDR built on the IAS in even-even $T_3 = 0$ nuclei has yet been reported besides our earlier work which spanned a limited range of excitation energy [3].

The importance of studying the GDR built on the $T = 1$ state in a $T_3 = 0$ nucleus arises from the following consideration. The GDR built on the ground state of $T = T_3 = 1$ nuclei exhibits isospin splitting. A $T = 1$ state, after absorbing a GDR photon, can be excited to $T = 0, 1$ or 2 states. In a $T_3 = 1$ nucleus, only $T = 1$ and 2 states are possible. These two components have been observed at two excitation energy regions [4] in many cases. For the $T = 1$ state in a $T_3 = 0$ nucleus, the GDR photon absorption can excite only the $T = 0$ and $T = 2$ components. The excitation of the $T = 1$ component is forbidden by the isospin selection rule for the isovector electric dipole transition. In the proton radiative capture reaction, both the target and the projectile have isospin 1/2. Assuming isospin purity in the entrance channel, the $T = 2$ component cannot also be excited. Thus these measurements allow a clean extraction of the $T = 0$ GDR component which can be compared with the $T = 1$ and $T = 2$ excitations in the $T_3 = 1$ analog nuclei.

The GDR built on the $T = 1$ ground state of ^{14}C studied via the photonuclear reaction [5] and the GDR on the $T = 1$ state in ^{14}N studied in the proton radiative capture reaction, show very different behaviors. The former shows broad GDR peaks at the excitation energies of ∼15 and 25 MeV. The latter does not show any peak but a broad variation of the cross section over the excitation energy range of ∼14 to 24 MeV. Since the $T = 1$ state in ^{14}N is at 2.31 MeV, the actual GDR energy (E_{GDR}) spans a range of ∼12 to 22 MeV. These observations imply different characters of the three GDR components built on the $T = 1$ state.

A guidance for the expected E_{GDR} on the 15.1 MeV state can be obtained from the following observations. The GDR built on the ground state of ^{14}N [2] shows a broad peak at an excitation energy of ∼22 MeV. The average value of E_{GDR} for the $T = 0$ component built on the $T = 1$ state is thus ∼5 MeV lower than that of the ground state GDR. The centroid energy of the GDR built on the ground state of ^{12}C is 22.6 MeV [6]. If E_{GDR} for the $T = 0$ component built on the 15.1 MeV state is lowered by a similar amount, then the excitation energy in ^{12}C for this component is at ∼32.5 MeV. This can be reached in the radiative capture reaction ^{11}B(p, γ) at $E_p \sim 18$ MeV. In our previous work [3], we have reported a measurement on this reaction leading to the 15.1 MeV state in ^{12}C at $E_p = 17$ to 24 MeV. A semidirect capture process exciting the GDR built on the 15.1 MeV state was used to describe the data. The E_{GDR} was inferred as ∼18.0 MeV which is 4.6 MeV lower than that of the ground state GDR. The derived width of ∼10.5 MeV was much larger than the widths [6] of GDR built on the ground and first excited states, viz., ∼3.3 MeV and 6.4 MeV, respectively. This implies that the GDR strength is spread over a wide range of excitation energies and only the higher energy part of this was measured earlier [3].

The present work reports a measurement of the proton radiative capture cross section to the 15.1 MeV state covering the E_p range of 7 to 24.5 MeV in steps of 0.5 to 1 MeV. The primary aim, as mentioned, was to extract the lower energy part of the $T = 0$ component of the GDR built on the $T = 1$ state. As in the case of ^{14}N, it will be interesting to compare this

component with the GDR built on the ground states of ^{12}B and ^{12}N in order to extract the characteristics of all three isospin components. Incidentally, the latter measurements have not yet been reported and can be carried out by a relativistic Coulomb excitation of the projectiles. The other consideration for the present measurement was the following. Besides our previous work, the only experiment on the radiative transition to the 15.1 MeV state was performed by Suffert *et al.* [7]. They observed a resonance at 18.1 MeV excitation in ^{12}C and assigned a magnetic dipole ($M1$) multipolarity to the $E_X = 18.1$ MeV to $E_X = 15.1$ MeV gamma transition. It is interesting to search for other $M1$ transitions to the 15.1 MeV state from the E_X region around 30 MeV. This is because the 15.1 MeV state qualifies as the giant $M1$ state built on the ground state [8,9] and the $E_X \sim 30$ MeV region, therefore, corresponds to the double giant $M1$ excitation. This excitation energy region in ^{12}C can be populated at $E_p \sim 15$ MeV in the ^{11}B(p, γ) reaction.

The basic experimental procedure was the same as that reported in our earlier work [3]. As mentioned earlier, a singles measurement is extremely difficult particularly to look for the transition to a high excitation energy of ∼15 MeV because of various extraneous sources contributing to the γ spectrum. Measurements were, therefore, made in coincidence with the 15.1 MeV to the ground state γ transition which has a branching ratio of ∼90%.

The experiment was performed with the proton beam from the Mumbai Pelletron accelerator bombarding a 98% enriched ^{11}B target of thickness ∼6.5 mg/cm^2. The energy loss of proton in the target was ∼0.3 MeV at 7 MeV and ∼0.1 MeV at 24 MeV. The proton beam was collimated in order to minimise the effect of the beam halo hitting the target frame. γ-rays were detected in two arrays of BaF_2 detectors each consisting of a close-packed group of seven elements and surrounded by a plastic anticoincidence shield. Each detector element was 20 cm long with a hexagonal cross section. The distance between the opposite faces of the hexagon was 6 cm in one array and 9 cm in the other. The detector arrays were kept close to the target at the distances of 7.7 cm (small array) and 9.4 cm (big array), the central axes of both the arrays being at 90° with the beam direction. Lead shields of about 10 cm thickness were placed on the top and two sides of each array. High density polypropylene and borated paraffin blocks were put near the beam collimators in order to reduce the neutron background. The beam dump was also shielded to reduce the γ-ray and neutron background.

The anode signal from the photomultiplier tube (PMT) of each BaF_2 detector was split and suitably amplified for individual energy, time and pileup measurements. For the energy and pileup measurements, the signal was fed to two charge sensitive analog to digital converters (QDC) with gate widths of 2 μs and 200 ns. The ratio of the two QDC outputs was used to detect the intradetector pileup in the off-line analysis. For the time measurement, the signal was fed to a low threshold (∼0.5 MeV) constant fraction discriminator (CFD). The CFD outputs were time matched within 0.4 ns and a logical OR signal for the full array was generated. The common gates of the QDCs were derived from this signal. The timings of the individual detectors in each array were measured with respect to the OR signal of the other array. The linear signals from all the detectors in an array were shaped with an integration time constant of ∼20 ns and summed for setting an overall high energy threshold to generate the trigger for data collection. The integration of the pulses before summing was necessary because the ratio of the fast to slow components was not identical in all the detector elements.

The energy calibration of the detectors was done using the 4.44 MeV, 6.13 MeV, and 15.1 MeV γ-rays from the ^{241}Am-Be, ^{239}Pu-^{13}C sources and the ^{12}C(p, p') reaction, respectively. For the inelastic scattering measurement, a proton beam of energy 19.6 MeV was used to bombard a polypropylene target of thickness 2.2 mg/cm^2. The high voltage on the PMTs of the BaF_2 detectors was chosen to ensure a linear energy response up to ∼ 35 MeV. The gain stability of the detectors was periodically monitored with the same radioactive sources and was found to be within ±0.5% over the period of experimental measurements.

The data were collected over a proton energy range of 7 to 24.5 MeV in 0.5 to 1 MeV steps, for an incident charge of ∼6 μC at each energy. Measurements with a blank target frame were made at a few energies in order to assess the problems arising from the beam hitting the upstream collimators. A computer based data acquisition system was used in an event by event mode. In each event, the parameters recorded were the twenty eight QDC outputs and fourteen timing outputs mentioned above.

An example of the time spectrum between the two arrays, with the condition of a total energy deposit ⩾9 MeV in each array, is shown in Fig. 1. In the off-line data analysis, a prompt time window (∼5 ns) was identified for each detector. The gate corresponding to no intradetector pileup was determined from the two-dimensional (2D) spectrum of the two QDC outputs.

In each event, the coincident detector groups of each array satisfying the conditions of no pileup and being in the prompt time windows were identified. The energy deposited in each group was summed to get the total energy in each array and a 2D energy spectrum was created at each beam energy. The chance coincidence contribution to the 2D spectrum generated using the multidetector arrays is not a straightforward issue. This was corrected for as follows. First, the probability of getting a chance coincidence event under the prompt peak for each detector was estimated from the counts under the prompt and the chance windows of the individual time spectrum. Then for each detector, satisfying the conditions for energy addition

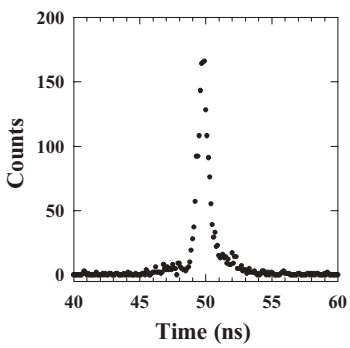

FIG. 1. Time spectrum between two detector arrays for an energy deposit of ⩾9 MeV in each.

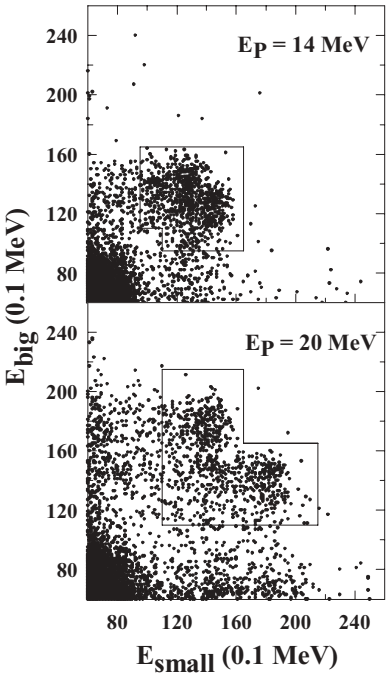

FIG. 2. Two dimensional γ-energy spectra with boron target at two beam energies. The contours show the energy windows used for extracting the coincidence yields.

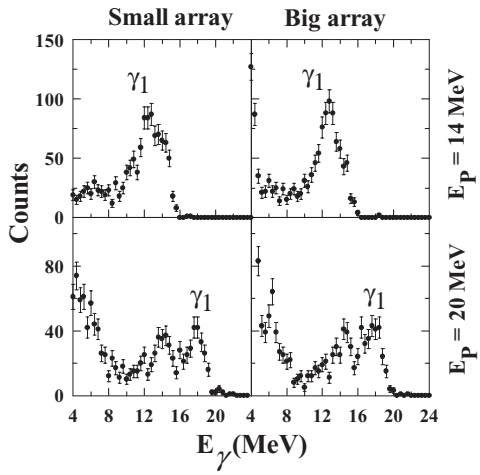

FIG. 3. Projected gamma spectra from the two-dimensional spectra in Fig. 2. The peaks due to the primary transitions (γ_1) are indicated.

elaborated above, a random number was generated and its energy was added to the total energy if the number was more than the above mentioned probability. The 2D energy spectrum thus generated corresponds to the true events. A comparison with the spectrum generated without this consideration gave the chance contribution.

Figure 2 shows examples of the 2D energy spectra with the boron target. The blobs corresponding to the coincidence between the primary (γ_1) and the 15.1 MeV γ-rays can be clearly seen. In the figure, the 15.1 MeV blob appears at a lower energy. This happens because the lower level thresholds in the QDCs were set at energies of 0.4 to 1.0 MeV in various detectors. The escape radiation of 0.511 MeV from one detector element to the neighboring one was, therefore, not included in the summed energy. This aspect was taken care of while calculating the energy response function of the arrays using the simulation program EGS4 [10]. The spectra measured with a blank target showed insignificant yield in the region of interest. Figure 3 shows the projected γ-spectra for both the arrays corresponding to an energy gate near 15.1 MeV in the coincident array. The peaks corresponding to the primary transition to the 15.1 MeV state can be clearly identified. The appearance of the peak/shoulder structures near 15.1 MeV is because the gates used in the projections contain events from the primary transition due to the response function of the detector arrays.

The γ-ray yields at various proton energies were extracted from the 2D chance-corrected spectra after using appropriate 2D energy windows shown by the contour lines in Fig. 2. The contribution from chance coincidences was $\sim$10% near $E_p =$ 7 MeV and $<$3% at higher beam energies. The efficiencies of the detector arrays for the selected energy windows were calculated by the program EGS4 for extracting the absolute cross sections. The target thickness was obtained by measuring the yield of 22.4 MeV γ-rays in the reaction $^{11}\mathrm{B}(p, \gamma_0)$ at $E_p = 7$ MeV. The measured thicknesses using data from both the detectors were consistent with each other within 3% with an average value of 6.5 mg/cm^2. The effect of the angular anisotropy between the cascading γ-rays on the extracted cross section was estimated in an approximate way described in our earlier paper. The effects are diluted (10 to 13%) because of the proximity of the detectors to the target. The attenuation of the γ-ray in the target chamber, the dead time correction for the acquisition system and the branching ratio for the ground state decay of the 15.1 MeV state were taken into account while extracting the absolute cross sections.

The extracted absolute cross sections as a function of proton energy are shown in Fig. 4(a). The error bars shown are statistical. The systematic error from other sources in the data analysis was estimated to be $<$12%. A major contribution to this is from the uncertainty in $\sigma(p, \gamma_0)$ which is used to extract the target thickness.

The direct-semidirect (DSD) model calculation has been elaborated in our earlier paper [3]. The results of the calculation for the GDR energy and width of 18.1 MeV and 11.0 MeV and the isovector potential $V_1 = 77.0$ MeV are shown by the solid line in Fig. 4(a). These values are within the error bars for the GDR energy and width fitting our earlier data, which are also shown in Fig. 4(b). The cross sections derived from the present measurement for $E_p = 17$ to 24 MeV agree reasonably with our earlier measurement.

In the 7 to 17 MeV range, the measured cross sections are very different from the DSD calculations and reveal two resonances. The data in this region can be fitted using a Breit-Wigner parametrization for the two resonances superimposed on a smooth background calculated using the DSD model. This is shown by the solid line in Fig. 4(b).

The extracted resonance parameters are shown in Table I. The four columns show the resonance energies in the center of mass (c.m.) system, the excitation energies in ^{12}C, the

TABLE I. Fitted resonance parameters.

$E_P^{\text{c.m.}}$ (MeV)	E_X (MeV)	$\Gamma^{\text{c.m.}}$ (MeV)	$(2J+1)\Gamma_{p0}\Gamma_\gamma/\Gamma$ (eV)
8.45±0.15	24.41 ± 0.15	1.3 ± 0.3	20.8 ± 2.8
12.85±0.10	28.81 ± 0.10	2.0 ± 0.2	150.0 ± 18.0

c.m. resonance widths and the resonance strengths $(2J+1)\,\Gamma_{p0}\Gamma_\gamma/\Gamma$, respectively. Here Γ_{p0} and Γ_γ are the partial widths for proton decay (to the ground state of ^{11}B) and gamma decay and Γ is the total width of the resonance with spin J. The extracted resonance parameters for other choices of linear smooth backgrounds are within the error bars shown in Table I.

If the multipolarity of the observed transitions from the resonances is electric quadrupole ($E2$), these would correspond to γ-decay widths $\Gamma_\gamma \geqslant 222/(2J+1)$ and $\geqslant 231/(2J+1)$ Weisskopf units (W.u.), respectively. Even for the highest possible resonance spin of $J=3$ in this case, the gamma widths are $\geqslant 31$ and $\geqslant 33$ W.u. for the two resonances. The actual values are more than these lower limits by a factor of Γ/Γ_{p0} which is expected to be $\gg 1$ considering the large number of possible decay channels. Even these lower limits are larger than the largest observed $E2$ strength of ∼8 W.u. [11] in ^{12}C or that allowed by exhaustion of the full sum rule strength [12] of the giant $E2$ resonance.

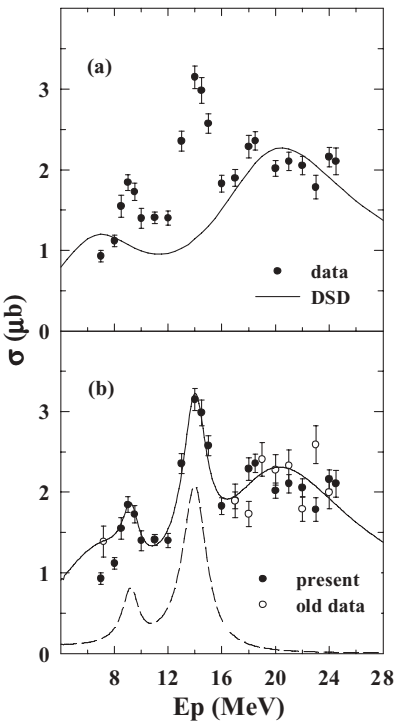

FIG. 4. (a) Measured radiative capture cross section at various proton energies. The solid line shows the results of the DSD model calculation (see text). (b) Comparison of the present and our old data [3]. The solid line shows the Breit-Wigner (BW) fits to the data superimposed on the DSD calculation in (a). The dotted line shows the contribution from BW resonances.

If the observed transitions have an $M1$ multipolarity, one can calculate the reduced transition strength $B(M1)\uparrow$ connecting the 15.1 MeV state to the resonances using the relations

$$B(M1)\downarrow = \frac{86.4}{E_\gamma^3}\Gamma_\gamma\downarrow, \tag{1}$$

$$\frac{B(M1)\uparrow}{B(M1)\downarrow} = \frac{2J+1}{2J_i+1}, \tag{2}$$

where Γ_γ is in eV, E_γ in MeV, $B(M1)$ in μ_N^2 (nuclear magneton squared), and $J_i(=1)$ is the spin of the 15.1 MeV state. These values are greater than 0.75 ± 0.10 and $1.70 \pm 0.20\ \mu_N^2$, respectively. Again the actual values are expected to be much larger considering the Γ/Γ_{p0} factor. The 15.1 MeV state is connected to the ground state by a strong $M1$ transition and corresponds to the giant $M1$ resonance built on the ground state [8,9]. From the known gamma decay width of the 15.1 MeV state [11] one gets $B(M1)\uparrow$ for this giant transition to be $2.85\ \mu_N^2$. As mentioned in the introduction, the $M1$ strength connected to the 15.1 MeV state at $E_X = 18.1$ MeV has been reported in Ref. [7]. The $B(M1)\uparrow$ value for this state can be calculated to be $\geqslant 2.95\ \mu_N^2$.

The sum rule limit for the $M1$ transition is defined as $\text{SRL} = \sum E_\gamma \times B(M1)\uparrow$, where the summation extends over all the states connected by the $M1$ transition to the initial state. The value of $E_\gamma \times B(M1)\uparrow$, in MeV. μ_N^2, for the transition from the ground state to 15.1 MeV state is 43.0 and that for the 15.1 MeV to 18.1 MeV state is >8.85. The $M1$ SRL is decided by the property of the initial state and is proportional to the expectation value $\langle \Sigma l.s \rangle$ of the nucleons, l and s referring the orbital and the spin angular momentum [9,13]. The ground state of ^{12}C has the predominant $p_{3/2}^4$ configuration whereas the 15.1 MeV state has the $p_{3/2}^3 p_{1/2}$ configuration. The magnitude of $\langle \Sigma l.s \rangle$ for the 15.1 MeV state should, therefore, be about a quarter of that for the ground state. Considering this, the 15.1 MeV to the 18.1 MeV transition should exhaust more than 80% of the corresponding SRL leaving about 20% for other transitions to exhaust. The values of $E_\gamma \times B(M1)\uparrow$ for the transition from the 15.1 MeV state to the present two resonances, in MeV. μ_N^2, are >7.0 and >23.3, respectively, exhausting >64% and >214% of the SRL. These high values strongly suggest that the observed transitions are not $M1$ in character. The present data, therefore, do not show any definite $M1$ resonance decaying to the 15.1 MeV state. An angular distribution measurement with higher statistics data can address the issue better.

The above arguments establish that the observed transitions from the resonances have electric dipole ($E1$) multipolarity. These correspond to gamma decay widths $\Gamma_\gamma > 0.073/(2J+1)$ and $>0.164/(2J+1)$ W.u., respectively. For the highest possible spin of $J=2$ in this case, the gamma widths are >14.5 and >32.8 mW.u. for the two resonances. The transition strengths imply that these are the components of the $T=0$ GDR built on the 15.1 MeV state. The present measurement establishes, therefore, a structured $E1$ strength distribution built on the 15.1 MeV state. This is very different from the GDR built on the $T=1$ state in ^{14}N and on the ground states of ^{12}C and ^{14}C. The excitation energies of

the structures, viz., ∼9.3 and 13.7 MeV above the 15.1 MeV state could correspond to the excitation of the $p_{1/2}$ nucleon of the 15.1 MeV configuration to the $s_{1/2}$ or $d_{3/2}$ states. The $E1$ strength lying at higher energies would correspond to the excitation of the $p_{3/2}$ nucleons to $s_{1/2}$, $d_{3/2}$, and $d_{5/2}$ states. It may be pointed out that the excitation of the $p_{3/2}$ and $p_{1/2}$ nucleons should also feature in the description of the GDR built on the low lying states in ^{14}C and ^{14}N although the observed features in various nuclei are so different. In this context it will be interesting to compare the present data on the $T = 0$ component with the hitherto unmeasured strength distribution for the $T = 1$ and 2 components. This requires the study of the GDR on the ground states of ^{12}B and ^{12}N, as mentioned in the introduction. This will complete the study of all the three isospin components. Finally, a comprehensive theoretical calculation of the isospin components of the GDR in p-shell nuclei, which can be tested rigorously against the experimental data, is required to have a full understanding.

In summary, the present paper reports a measurement of the radiative proton capture to the 15.1 MeV $T = 1$ state in ^{12}C over a proton energy range of 7 to 24.5 MeV. The prominent features in the measured cross section are two resonances at excitation energies of ∼24.4 and 28.8 MeV superimposed on a smooth excitation function. The $E2$ or $M1$ multipolarity for the gamma decay from the resonances can be discarded on the basis of their transition strengths. The present experiment establishes a structured $T = 0$ $E1$ strength distribution built on the $T = 1$ state. This is very different from the GDR built on the $T = 1$ state in ^{14}N and on the ground state ^{12}C and ^{14}C. A measurement of the electric dipole strength distribution built on the ground states of ^{12}B and ^{12}N will complete the experimental study of all the isospin components of the GDR in $A = 12$ isobars. The apparently different features of the GDR strength distribution built on the $T = 0$ and $T = 1$ states in the p-shell nuclei can be fully understood only through a comprehensive theoretical calculation.

We thank W. R. Lozowski for providing the ^{11}B target, the Mumbai Pelletron staff for accelerator operation, R. Kujur, M. Pose, and Y. Sawant for their help during the experiment and M. N. Harakeh and J. P. Schiffer for their valuable comments.

[1] M. B. Johnson and C. L. Morris, Annu. Rev. Nucl. Part. Sci. **43**, 165 (1993), and references therein.
[2] P. Paul, H. S. Kuan, and E. K. Warburton, Nucl. Phys. **A254**, 1 (1975).
[3] D. R. Chakrabarty, V. M. Datar, Suresh Kumar, E. T. Mirgule, A. Mitra, V. Nanal, and H. H. Oza, Phys. Rev. C **69**, 021602(R) (2004).
[4] P. Paul, F. Amann, and K. A. Snover, Phys. Rev. Lett. **27**, 1013 (1971).
[5] S. S. Dietrich and B. L. Berman, At. Data Nucl. Data Tables **38**, 199 (1988).
[6] R. G. Allas *et al.*, Nucl. Phys. **58**, 122 (1964).
[7] M. Suffert, W. Feldman, and S. S. Hanna, Part. & Nuclei **4**, 175 (1972).
[8] S. Hanna, in *Isopin in Nuclear Physics* edited by D. H. Wilkinson (North Holland, Amsterdam, 1969), p. 593.
[9] D. Kurath, Phys. Rev. **130**, 1525 (1963).
[10] W. Nelson, H. Hirayama, and D. Roger, Stanford University Report SLAC-265, 1985.
[11] F. Ajzenberg-Selove, Nucl. Phys. **A506**, 1 (1990).
[12] H. R. Weller and N. R. Roberson, Rev. Mod. Phys. **52**, 699 (1980).
[13] M. Traini, Phys. Rev. Lett. **41**, 1535 (1978).